ACI STRUCTURAL JOURNAL TECHNICAL PAPER

Title no. 110-S52

# Tension-Stiffening Model for Steel Fiber-Reinforced Concrete Containing Conventional Reinforcement

by Seong-Cheol Lee, Jae-Yeol Cho, and Frank J. Vecchio

*The tensile behavior of fiber-reinforced concrete (FRC) members co-reinforced with conventional deformed reinforcing bar (R/FRC members) is analytically investigated in regards to tensile stresses developed in the reinforcing bars, tensile stresses induced in the steel fibers bridging a crack, and the bond mechanism between the reinforcing bar and the concrete matrix. A tension-stiffening model for R/FRC members is developed through an analytical parametric study using a crack analysis procedure that considers the tensile behavior due to the steel fibers and the bond stress-slip relationship between the reinforcing bar and the concrete matrix. With the proposed model, the local yielding of reinforcing bars at a crack can be realistically simulated, enabling reasonably accurate predictions of the tensile behavior of R/FRC members. Analysis results obtained from the proposed model show good agreement with the test results measured by previous researchers.*

**Keywords:** bond; crack; steel fiber; steel fiber-reinforced concrete (SFRC); tension; tension stiffening.

## INTRODUCTION

Steel fibers are used in concrete structures to partially compensate for the innate low tensile strength and brittle tensile response of the concrete. For the last several decades, many researchers[1-6] have demonstrated through direct tensile tests that fiber-reinforced concrete (FRC) members can exhibit ductile behavior, even after cracking. Recently, several theoretical models[7-10] have been developed to predict the tensile behavior of FRC members subjected to uniaxial tension. Some[7,8] are based on the assumption that a constant bond stress is developed along the fiber. The Diverse Embedment Model (DEM),[9,10] on the other hand, considers both uniform frictional bond stresses and mechanical anchorage effects in modeling the pullout behavior of a steel fiber. In addition, the random distribution of fibers is also considered in the DEM so that the tensile behavior of FRC members with straight or hooked-end fibers can be more realistically simulated. With respect to experimental investigations aimed at evaluating the tensile behavior of FRC members, the majority have focused on members containing steel fiber only. Studies of the tensile behavior of FRC members with conventional reinforcements (R/FRC) have been less common. Yet, in most practical applications of FRC construction, structural members are typically co-reinforced with conventional reinforcing bar.

The tension behavior of R/FRC members is substantially different from that of conventional reinforced concrete (RC) members, as shown in Fig. 1. Figure 1 illustrates the basic differences in behavior between RC and R/FRC members. In the tensile behavior of an RC member beyond the initial cracking point, the overall response gradually approaches that of the bare bar; as yielding of the reinforcing bar is reached, little or no increase in tensile strength and stiffness will remain over the bare bar response.[11] In the tensile behavior of an R/FRC member, on the other hand, higher tensile stresses can be resisted not only after initial cracking but also after yielding of the reinforcing bar because the contribution of fibers to the tensile stress is considerable. In addition, the average crack spacings and crack widths in R/FRC members are smaller than those in RC members.

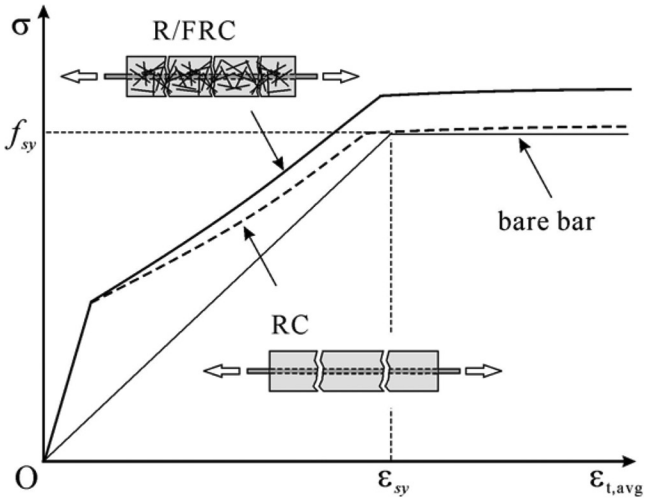


*Fig. 1—Tensile behavior of RC and R/FRC members.*

Recently, several researchers[12-17] have investigated the tensile behavior of R/FRC members. However, while most researchers[12-14,17] have focused on test results obtained from experiments on R/FRC members subjected to uniaxial tension, only a few theoretical approaches[12,15,16] have been developed to evaluate the tension-stiffening effect in R/FRC members. In these models, because the previous tension-stiffening models for R/FRC members evaluate only the total tensile stress of the matrix—combining the fiber and concrete contributions and representing the difference between the total response of an R/FRC member and that of a bare bar—the tensile stresses due to fibers and the bond mechanism between the concrete matrix and the reinforcing bar cannot be separately evaluated. To be able to do so is important in calculating the difference between the average tensile stress and the local stress in a reinforcing bar which, in turn, is used for checking the local equilibrium and the calculation of the shear slip at a crack[18-20] because reinforcing

*ACI Structural Journal*, V. 110, No. 4, July-August 2013.

*ACI member* **Seong-Cheol Lee** *is an Assistant Professor at KINGS, South Korea. He received his PhD from Seoul National University, Seoul, Korea, in 2007. His research interests include the shear behavior of concrete structures and the analysis of prestressed concrete structures and fiber-reinforced concrete members.*

*ACI member* **Jae-Yeol Cho** *is an Assistant Professor in the Department of Civil & Environmental Engineering at Seoul National University. He received his PhD from Seoul National University. His research interests include nonlinear analysis and optimized design of reinforced and prestressed concrete structures, material modeling, and similitude laws for the dynamic test of concrete structures.*

**Frank J. Vecchio**, *FACI, is a Professor in the Department of Civil Engineering at the University of Toronto. He is a member of Joint ACI-ASCE Committees 441, Reinforced Concrete Columns, and 447, Finite Element Analysis of Reinforced Concrete Structures. His research interests include nonlinear analysis and design of reinforced concrete structures, constitutive modeling, performance assessment and forensic investigation, and repair and rehabilitation of structures.*

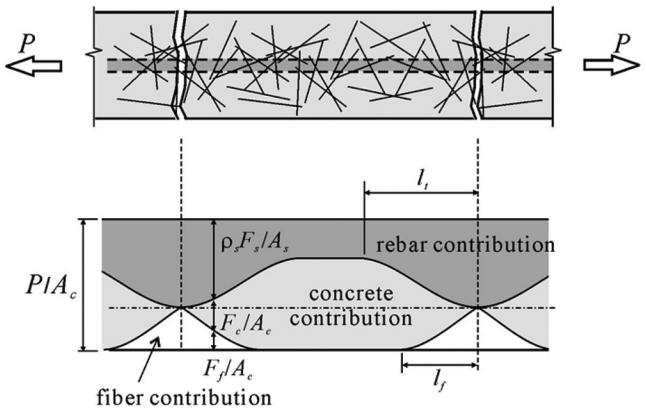


*Fig. 2—Distribution of stresses between cracks in R/FRC members.*

bar stress varies between cracks. In other words, the tensile stress near the yielding of the reinforcing bar cannot be evaluated exactly. Consequently, the currently available tension-stiffening models for R/FRC members cannot be appropriately employed with analysis models,[18-20] sectional analysis procedures,[21] and finite element analysis procedures[22-24] based on the Smeared Crack Model.

In this paper, a tension-stiffening model is derived to realistically reflect the effect of steel fibers on the tensile behavior of R/FRC members—doing so by evaluating the tensile stress due to bond mechanisms between a reinforcing bar and the surrounding concrete matrix in which the tensile stress attained by fibers is not included. The derivation is based on the DEM, a rational mechanistic model recently developed to predict the tensile behavior of FRC members.

## RESEARCH SIGNIFICANCE

A rational tension-stiffening model has been developed to evaluate the tension-stiffening effect in R/FRC members. With the proposed model, considering both the apparent average tensile stress-strain behavior and the local yielding of the reinforcing bar at a crack, a more realistic calculation of the tensile behavior of R/FRC members is possible. The proposed tension-stiffening model can easily be implemented in most analysis procedures,[18-24] such that it will be useful in simulating the structural behavior of R/FRC members because, in most practical structural applications of FRC, fibers are used in combination with conventional reinforcement.

## ANALYSIS FOR UNIAXIAL TENSILE BEHAVIOR OF R/FRC MEMBERS

The crack analysis procedure previously developed by Lee et al.,[11] based on work by Balázs[25] and Oh and Kim,[26] will be extended to tensile behavior analysis of R/FRC members subjected to uniaxial tension. In this section, the crack analysis procedure is summarized with particular attention given to the tensile stresses attained by steel fibers and their distribution between cracks. In considering the contribution of steel fibers on the tensile behavior, the DEM[9,10] is adopted. For verification, the analysis results computed by the proposed crack analysis procedure are compared with results from experiments on R/FRC members.[14,17] The procedure is later employed to develop a tension-stiffening model for R/FRC members.

### Local behavior of R/FRC members between cracks

In FRC members, unlike with conventional RC members, a considerable amount of concrete tensile stress is transmitted across a crack because of steel fibers bridging the crack. Thus, in R/FRC members, the contribution of steel fibers should be explicitly considered in explaining the distribution of concrete tensile stresses—at the crack and between cracks—in addition to the contributions from the concrete matrix and the reinforcing bar. Figure 2 illustrates the distribution of the tensile stress components between cracks. In this study, the contributors to tensile stress resistance in FRC have been divided into two components: one due to steel fibers, which can be analytically evaluated using the DEM[9,10]; and the other due to the concrete matrix, which can be calculated by removing the contribution of steel fibers from the total tensile stress.

As illustrated in Fig. 2, the tensile stress in the concrete matrix varies from zero at a crack to the maximum between cracks because the tensile stresses sustained by steel fibers and reinforcing bar at the crack are transmitted to the concrete matrix between the cracks. Consequently, two tensile resistance mechanisms can be considered after cracking: the tensile stress carried by steel fibers and the bond mechanism between the concrete matrix and the reinforcing bar. As shown in the figure, the distribution of the tensile stress in the reinforcing bar is affected predominantly by the bond mechanism between the concrete matrix and the reinforcing bar, not by the distribution of the tensile stress due to steel fibers. Therefore, the basic assumption for the formulation presented in this paper is that the tensile stress due to the tension-stiffening effect in R/FRC members can be derived solely from the bond mechanism between the concrete matrix and the reinforcing bar; the tensile stress carried by steel fibers is not included in the tension-stiffening effect but is treated separately. Thus, it is possible to evaluate the difference between the average and local tensile stresses of the reinforcing bar.

### Crack analysis procedure for R/FRC members subjected to uniaxial tension

The equilibrium condition for an infinitesimal element in R/FRC members subjected to uniaxial tension can be considered as shown in Fig. 3. Unlike conventional RC members, the distribution of tensile stress due to steel fibers should be considered in the equilibrium relation. Hence, the equations of equilibrium can be derived as follows

$$\tau_b d_{bs} \pi dx = df_s A_s \quad (1)$$

$$\tau_b d_{bs} \pi dx - df_f A_c = df_c A_c \tag{2}$$

From the definition that the local slip is the difference of the deformation between the concrete matrix and the reinforcing bar, the equations for the compatibility can be derived as follows

$$s = u_s - u_c \text{ or } s'' = \frac{d\varepsilon_s}{dx} + \frac{d\varepsilon_c}{dx} \tag{3}$$

From Eq. (1) through (3), the governing equation for the local behavior of R/FRC members subjected to uniaxial tension can be derived as follows

$$s'' = \frac{\tau_b d_{bs} \pi}{E_s A_s} + \frac{\tau_b d_{bs} \pi}{E_c A_c} - \frac{1}{E_c} \frac{df_f}{dx} \tag{4}$$

As a constitutive law to solve the governing equation, the bond stress-slip relationship between the reinforcing bar and the FRC matrix presented in the following equation[27] was adopted. Note that the effect of concrete splitting was ignored because splitting cracks were not observed in the tests up to the yielding of the reinforcing bar.[17]

$$\tau = \tau_{max} \left( \frac{s}{s_1} \right)^{0.3} \quad \text{for } s \le s_1 \tag{5}$$

where $\tau_{max} = 2.57\sqrt{f_c'}$ in MPa; and $s_1$ is 1.5 mm (0.06 in.).

The governing equation cannot be explicitly solved—even for the initial cracking stage—because of the term reflecting the distribution of the tensile stress due to steel fibers. Hence, the fourth-order Runge-Kutta Method, a numerical procedure applicable to second-order differential equations that employs the derivative at a section to extrapolate the solution to the next section, has been employed to calculate the transfer length at the initial cracking stage. The transfer length $l_t$, over which the stress of the reinforcing bar and that attained by steel fibers can be transferred to the concrete, will then be used for the calculation of average crack spacing at initial cracking in an R/FRC member subjected to uniaxial tension.

The average crack spacing at initial cracking was assumed as $4l_t/3$, as suggested in CEB-FIP MC90.[28] Because the transfer length increases with increasing tensile stress in the reinforcing bar at a crack, the cracking behavior of members subjected to uniformly distributed uniaxial tension should progress to the stabilized crack formation stage after the first cracking phase. For additional cracks with increasing tensile load, it can be assumed that a new crack will form midway between two adjacent cracks, where the concrete stress is greatest. Because an explicit mathematical solution is not possible, the fourth-order Runge-Kutta Method has again been employed.

The local strain in the reinforcing bar at a crack can exceed the yield strain even when the average tensile strain is less than the yield strain. Thus, the effects that large tensile strains in a reinforcing bar have on the bond stress should be considered when modeling tension stiffening; moreover, they should be considered after the average yielding of the reinforcing bar and not only before, as is usually done. To consider the decrease in bond efficiency caused by the lateral contraction of a reinforcing bar due to its large tensile strain, the following bond coefficient,[29] which is to be multiplied by the bond stress obtained from Eq. (5), has been used

$$K_b(\varepsilon_s) = \exp\left\lfloor \min\left\{0,\ 10\left(\varepsilon_{sy} - \varepsilon_s\right)\right\}\right\rfloor \tag{6}$$

The analysis algorithm for the crack analysis procedure is presented in Fig. 4. As shown in the figure, the transfer length is first evaluated to calculate average crack spacing at an initial cracking. Then, by satisfying the compatibilities regarding the crack width and the tensile stress of concrete matrix at a crack, which are consequences of the pre-assumed values, the tensile behavior of an R/FRC member can be analyzed.

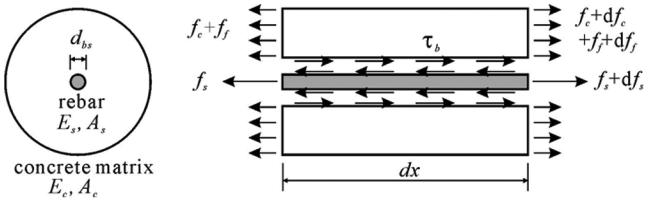


*Fig. 3—Infinitesimal element subjected to axial tension.*

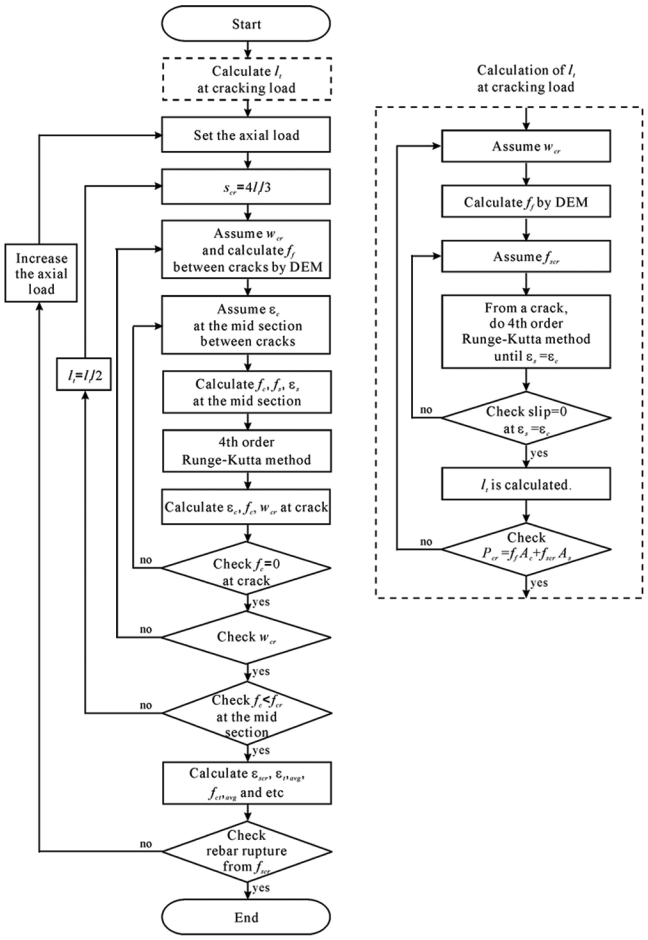


*Fig. 4—Algorithm of crack analysis procedure for R/FRC members.*

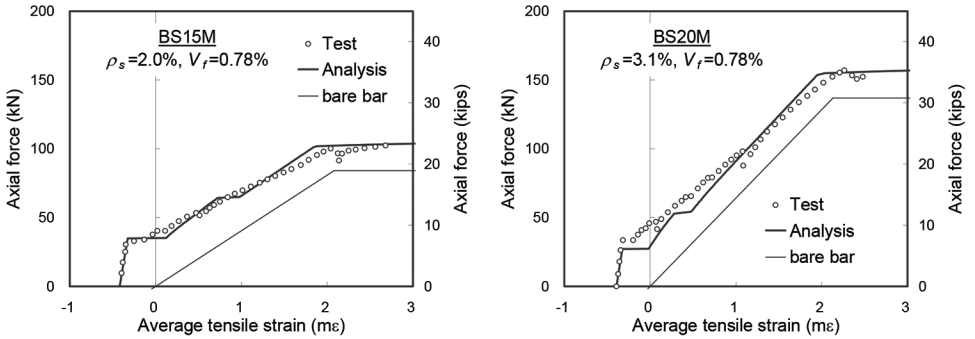


*Fig. 5—Comparison of test results and calculated responses obtained from proposed crack analysis procedure.*

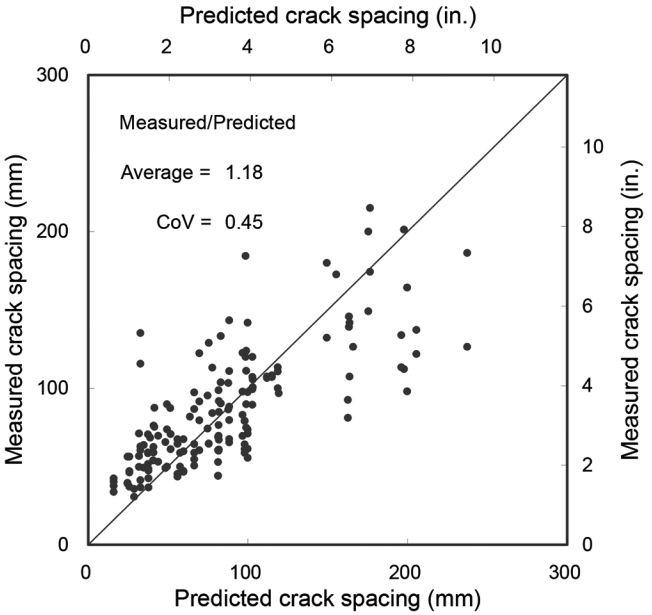


*Fig. 6—Comparison of average crack spacing.*

## Verification of crack analysis procedure

For verification of the crack analysis procedure presented in the previous section, data from R/FRC members tested by Bischoff[14] have been compared with the analysis results. A comparison of the relationships between the applied tensile force and the average tensile strain are presented in Fig. 5. Because the concrete shrinkage is considered, the average tensile strain is negative at the beginning of the relationship. It should be noted that the tensile behavior after yielding of the reinforcing bar can be used for verification of whether the DEM reasonably evaluates the tensile force attained by steel fibers because the tension-stiffening effect quickly diminishes as yielding of the reinforcing bar is reached. In addition, the tensile behavior before the yielding of the reinforcing bar can be used for verification of whether the crack analysis procedure sufficiently models the tension-stiffening effect. Through a comparison between the experimental and calculated responses shown in Fig. 5, it can be concluded that the crack analysis procedure predicts the tension-stiffening effect in the pre-yield tensile behavior of R/FRC members well. In addition, it can be seen from a comparison of the post-yield tensile behavior that the DEM accurately captures the tensile force sustained by the steel fibers.

Deluce and Vecchio[17] tested a comprehensive series of 48 uniaxially stressed R/FRC specimens; the average crack spacings reported for these tests were compared with corresponding calculated values obtained from the crack analysis procedure presented. It should be noted that the average crack spacing is important in the prediction of the tensile behavior of R/FRC members because the tensile stress attained by steel fibers is evaluated for a given crack width, which is obtained from multiplying the average tensile strain in the R/FRC member by the average crack spacing. As shown in Fig. 6, the calculated values show reasonably good agreement with the measured average crack spacings. Although the results are scattered, this is mainly due to the assumption in the crack analysis procedure that the average crack spacing is halved and the number of cracks doubled when the tensile stress of the concrete matrix between cracks reaches the cracking strength; the actual observed progression of cracking is more gradual and sequential.

Thus, based on the results of the axial tensile force-strain responses and the average crack spacings obtained, it can be concluded that the crack analysis procedure presented in this study can be used for reasonable evaluations of the tension-stiffening effect in R/FRC members.

## Investigation of tension-stiffening effect

Using the crack analysis procedure described in the previous section coupled with the DEM, the total tensile stress response of an R/FRC member can be found as the sum of the stress components due to the reinforcing bar, the steel fibers, and the bond mechanism of the reinforcing bar. The average tensile stress of the reinforcing bar can be calculated sufficiently well using a bilinear (elasto-plastic) relationship. The tensile stress carried by the steel fibers can be calculated for a given crack width using the DEM. Because the tensile stress attained by steel fibers is transmitted only to the concrete matrix, as illustrated in Fig. 2, the tensile stress attained by steel fibers at a crack can be used for the portion due to fibers. The tensile stress due to the bond behavior of the reinforcing bar, which is defined as the tension-stiffening effect in this paper, can be extracted from the total response by removing the tensile stresses due to the reinforcing bar and steel fibers. Therefore, the difference between the average tensile stress of the reinforcing bar and the tensile stress of the reinforcing bar at a crack can be directly calculated from the tensile stress due to the tension-stiffening effect.

Figure 7 shows the analysis results for the three components in the tensile behavior of the two R/FRC members

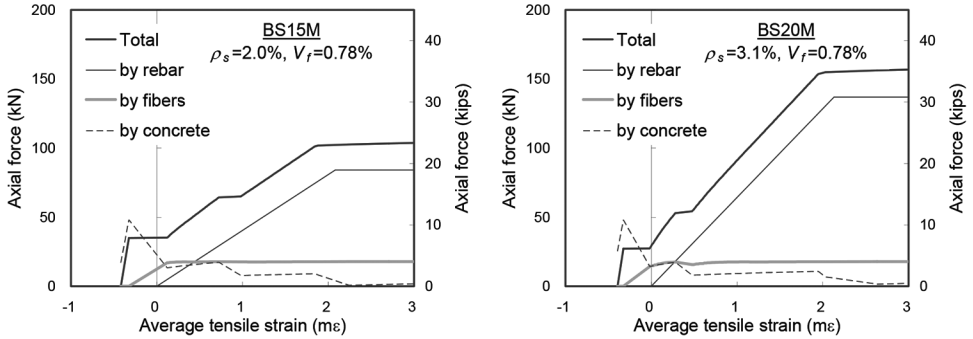


*Fig. 7—Component forces in tensile behavior of R/FRC members calculated by crack analysis procedure.*

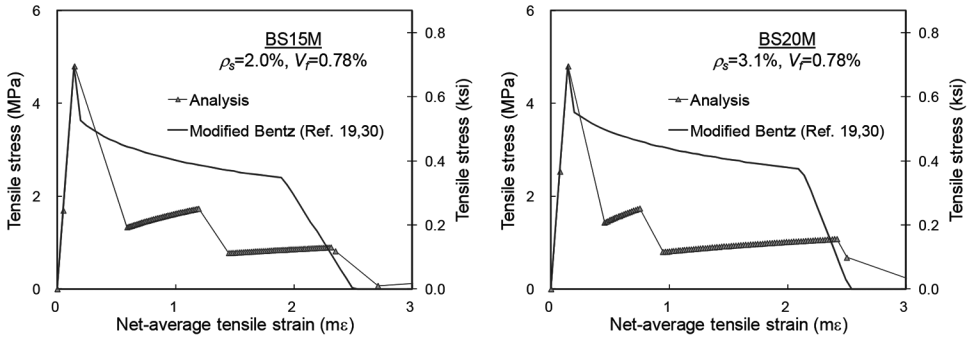


*Fig. 8—Comparison of crack analysis results and conventional tension-stiffening model.*

tested in uniaxial tension by Bischoff.[14] As seen in the figure, the tensile stress carried by the steel fibers increases with increasing axial deformation after initial cracking. On the other hand, the tensile stress due to the tension-stiffening effect (that is, the concrete component) decreases after local yielding of the reinforcing bar because of the local equilibrium requirement at a crack by the following equation

$$f_{c,TS} = \rho_s \left( f_{scr} - f_{s,avg} \right) \tag{7}$$

where $f_{scr} \le f_{sy}$.

After the average tensile strain of the member reaches the yield strain of the reinforcing bar, the tension-stiffening effect has largely diminished. Hence, the total tensile stress of R/FRC members after yielding of the reinforcing bar approaches the sum of the bare response and the tensile stress sustained by the steel fibers.

The calculated tensile stress due to tension stiffening in R/FRC was compared with that determined from a finite element analysis[24] using a formulation that has shown good accuracy for RC members without steel fibers.[19,30] As seen in Fig. 8, without rational consideration of steel fibers, the tension-stiffening model for RC members significantly overestimates the tension-stiffening effect. In addition, the tensile stress of the reinforcing bar at a crack can also be overestimated by Eq. (7). In reality, the tension-stiffening effect must be smaller in R/FRC members because more numerous smaller-width evenly distributed cracks are developed relative to the cracking seen in similar RC members. From the results presented in Fig. 5 and 8, it can be concluded that the tension-stiffening effect in R/FRC members subjected to uniaxial tension can be more reasonably evaluated by the crack analysis procedure presented in this study.

## DEVELOPMENT OF TENSION-STIFFENING MODEL FOR R/FRC MEMBERS

Based on the crack analysis procedure presented in the previous section, an analytical parametric study was conducted to derive a tension-stiffening model that more accurately reflects the effect of steel fibers. In this study, the conventional tension-stiffening model for RC members[30] was modified to take into account the effect of steel fibers as follows

$$f_{c,TS} = \frac{f_{cr}}{1 + \sqrt{3.6\, c_f M\, \varepsilon_{t,avg}}} \tag{8}$$

where $c_f$ is the coefficient to consider the effect of steel fibers. The bond parameter $M$ is calculated from $M = A_c / \left( \sum d_{bs} \pi \right)$ in mm.

In the following section, the parametric study presented was focused on the evaluation of $c_f$.

### Analytical parametric study on tension-stiffening effect in R/FRC members

The variables considered in the parametric study were: percentage of conventional reinforcement (1.33, 1.56, 1.75, 3.00, 3.11, and 4.00%); fiber volumetric ratio (0.5, 1.0, and 1.5%); and fiber type in accordance with the previous experimental program.[17] The characteristics of the steel fibers considered in the parametric study are presented in Table 1. Neither concrete compressive strength nor reinforcing bar yield strength were considered in the study because they have little influence on the tension-stiffening response, as can be deduced from Fig. 9, where the predicted tension-stiffening effects almost coincide until the average strain reaches approximately 0.002. In the parametric study, the compressive

strength of concrete was fixed at 60.0 MPa (8.70 ksi) and the direct tensile strength was taken as 2.56 MPa (0.37 ksi) from the relationship $f_{cr} = 0.33\sqrt{f_c'}$ (MPa), which is commonly adopted in the analysis of concrete members.[22] The elastic modulus of the concrete was estimated to be 32,500 MPa (4710 ksi) from $E_c = 3300\sqrt{f_c'} + 6900$ (MPa), as presented in CSA A23.3-04[31] because it is known that the inclusion of steel fibers has only a minor influence on the initial elastic modulus for specimens in which the casting direction is parallel to the crack surface.[32] The yield strength and Young's modulus of the reinforcing bar were assumed to be 500 and 200,000 MPa (72.5 and 2901 ksi), respectively.

**Table 1—Characteristics of hooked-end steel fibers**

| Type | Length, mm (in.) | Diameter, mm (in.) | Aspect ratio | Tensile strength, MPa (ksi) |
|---|---|---|---|---|
| Type 1 | 30.0 (1.18) | 0.38 (0.015) | 78.9 | 3100 (450) |
| Type 2 | 30.0 (1.18) | 0.55 (0.022) | 54.5 | 1245 (181) |
| Type 3 | 50.0 (1.97) | 1.05 (0.041) | 47.6 | 1100 (160) |

Figure 10 summarizes the results of the parametric study for each of the three previously identified variables. From the bond parameter results presented in Fig. 10(a), one is able to see the influence of the reinforcement ratio on the tension-stiffening effect. It is noted that the bond parameter was controlled by varying the reinforcing bar diameter and

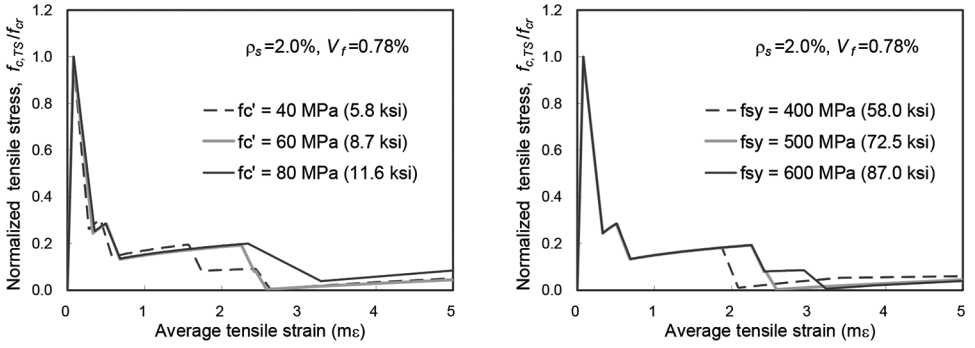


*Fig. 9—Influence on concrete tensile stress due to tension stiffening: (a) concrete compressive strength; and (b) reinforcing bar yield strength.*

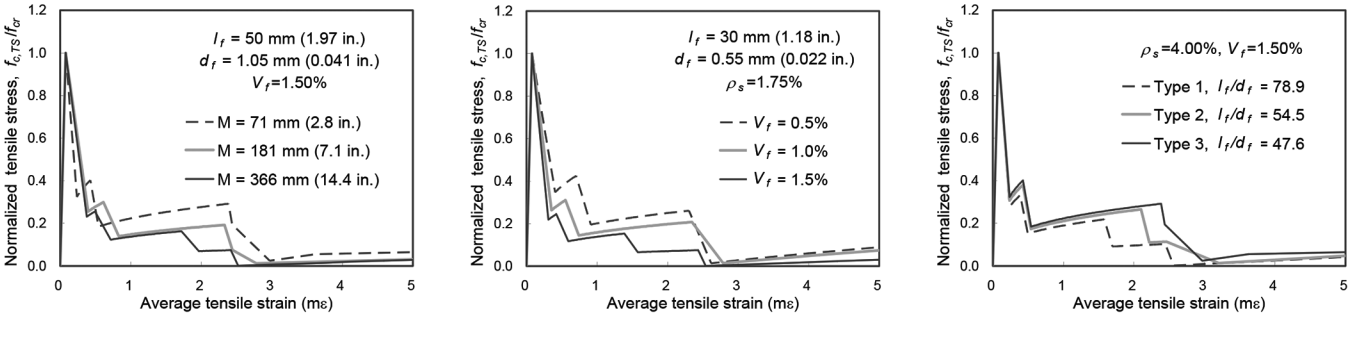


*Fig. 10—Effect of variables on tension-stiffening effect: (a) bond parameter; (b) fiber volumetric ratio; and (c) steel fiber type.*

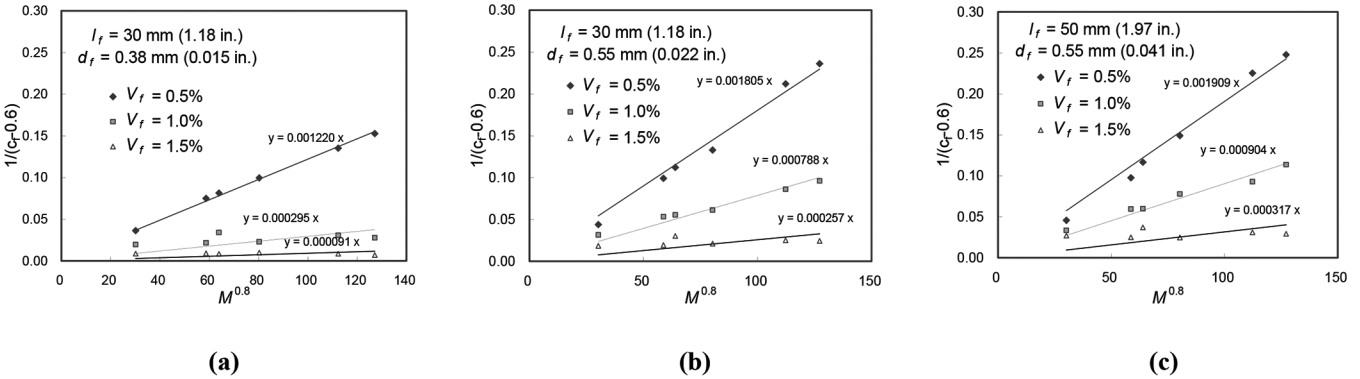


*Fig. 11—Relationship between bond parameters* $c_f$ *and* M*: (a) Fiber Type 1; (b) Fiber Type 2; and (c) Fiber Type 3.*

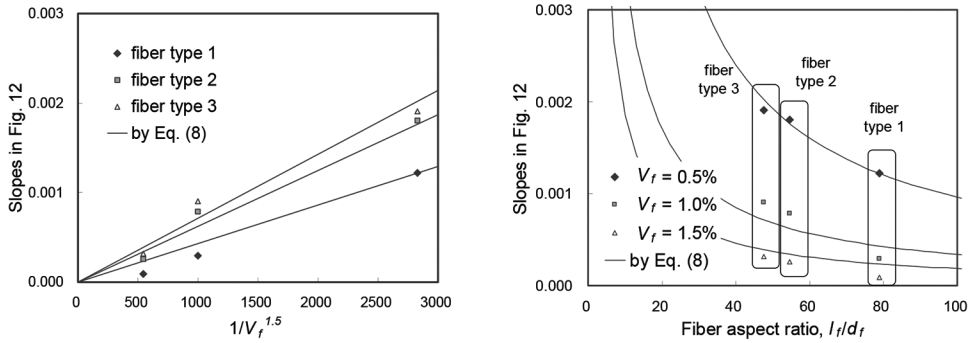


**(a)** **(b)**

*Fig. 12—Effect of variables on slopes in Fig. 11: (a) fiber volumetric ratio; and (b) fiber aspect ratio.*

the reinforcement ratio through the parametric analyses. As shown in this figure, the tension-stiffening effect due to the bond mechanism between the concrete matrix and the reinforcing bar increases with a decrease in the bond parameter. This result coincides with the common observation that the tension-stiffening effect is greater in RC members with a larger reinforcement ratio and a smaller reinforcing bar diameter. On the other hand, the tension-stiffening effect decreases with an increasing fiber volumetric ratio and the fiber aspect ratio (refer to Fig. 10(b) and (c)). This result can also be explained by the fact that the crack spacing becomes smaller with the increasing contribution of steel fibers to the tensile behavior.

### Tension-stiffening model for R/FRC members

From the analysis results obtained from the crack analysis procedure through the parametric study as presented in Fig. 10, $c_f$ in Eq. (8) can be calculated at every analysis point. Then, for a given R/FRC member, the representative value of $c_f$ can be evaluated by averaging the values for all analysis points between initial cracking and local yielding of the reinforcing bar because the tensile stress due to the tension-stiffening effect linearly decreases after local yielding to meet the local equilibrium requirement expressed by Eq. (7). As presented in Fig. 11, the term $(c_f - 0.6)$ was used instead of $c_f$ to investigate the effect of the variables considered in the parametric study because $c_f$ is known to be 0.6 for conventional RC members.[21] Through the parametric analyses, as shown in the figure, it was found that a linear relationship between $1/(c_f - 0.6)$ and $M^{0.8}$ can be assumed. Figure 12 shows that linear and inverse-proportional relationships adequately capture the effects of the fiber volumetric ratio and the fiber aspect ratio, respectively, on the slopes presented in Fig. 11. From the figures, it is proposed that $c_f$ for R/FRC members with hooked-end steel fibers be defined as follows

$$c_f = 0.6 + \frac{1}{0.034}\left(\frac{l_f}{d_f}\right)\frac{\left(100V_f\right)^{1.5}}{M^{0.8}} \quad \text{for hooked-end fibers} \tag{9a}$$

In the same manner as for hooked-end steel fibers, an equation for $c_f$ for hooked-end fibers for R/FRC members with straight fibers is developed as follows

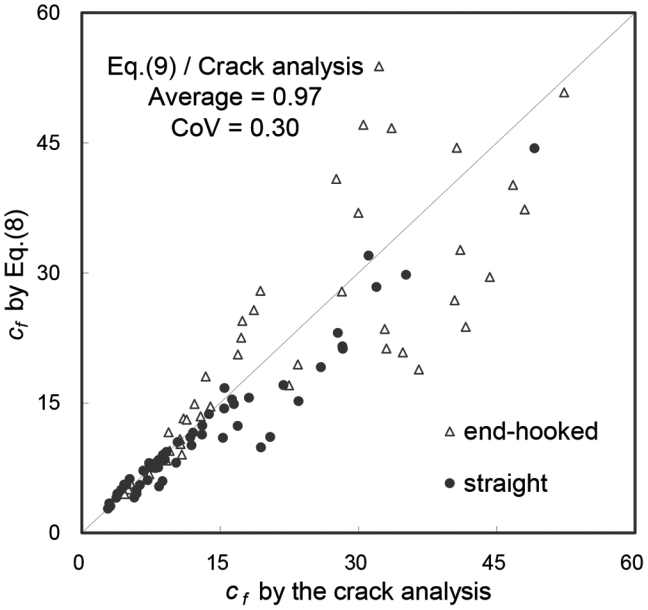


*Fig. 13—Comparison of Eq. (9) and prediction of crack analysis procedure.*

$$c_f = 0.6 + \frac{1}{0.058}\left(\frac{l_f}{d_f}\right)^{0.9}\frac{100V_f}{M^{0.8}} \quad \text{for straight fibers} \tag{9b}$$

In the parametric study for straight fibers, only the pullout strength was reduced in the calculation of the tensile stress attained by fibers based on the DEM; all other conditions were the same as for hooked-end fibers.

Figure 13 compares the values of the coefficient $c_f$ calculated by Eq. (9) with those determined from the crack analysis procedure. It can be concluded that Eq. (9) reflects the effect of steel fibers on the tension stiffening for both straight and hooked-end fibers well. Although some scatter is seen at large values of $c_f$, it is not of major concern because the tensile stress due to the tension-stiffening effect calculated by Eq. (8) and (9) shows good agreement with those evaluated by the crack analysis procedure; for example, the mean and standard deviation were 0.964 and 0.062, respectively, for the ratio of the tensile stress due to the tension-stiffening effect at the average tensile strain of 0.001.

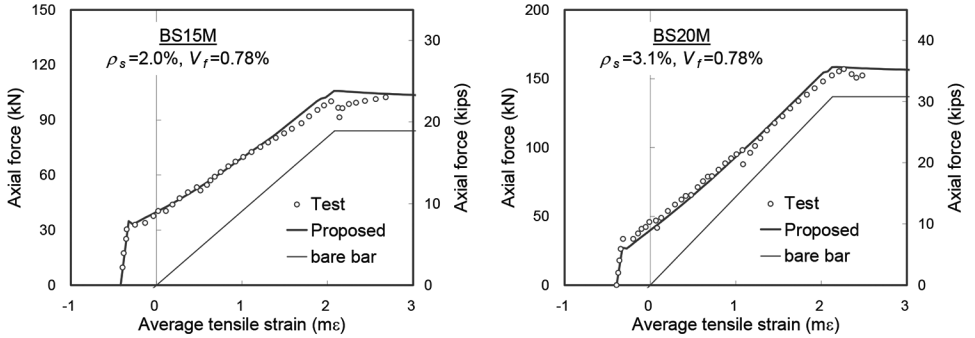


**(a)**

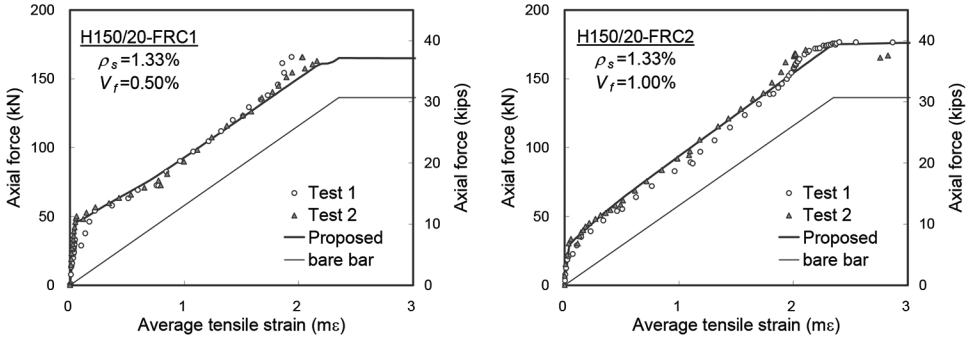


**(b)**

*Fig. 14—Comparison of proposed model and test results by: (a) Bischoff[14]; and (b) Deluce and Vecchio.[17]*

## VERIFICATION OF PROPOSED TENSION-STIFFENING MODEL

For validation of the proposed tension-stiffening model, several R/FRC members tested by previous researchers[14,17] were analyzed. In the analysis, the DEM[9,10] was employed for the evaluation of the tensile stresses developed by the steel fibers. In addition, the tensile stresses due to concrete tension-softening effects should also be taken into account. In this study, the following exponential function was adopted for the tension-softening effect of the concrete matrix[8]

$$f_{c,soft} = f_{cr} e^{-15 w_{cr}} \tag{10}$$

In the analysis of RC members using the Disturbed Stress Field Model (DSFM),[19,20] the average tensile stress of concrete matrix is determined to be the tensile stress due to the tension-softening effect or the tension-stiffening effect, whichever is larger. Similarly, in the analyses of R/FRC members, the tensile stress resistance contributed by the reinforcing bar and the steel fibers is added to the tensile stress calculated from Eq. (8) and (9) or Eq. (10), whichever is larger.

Because the tensile stresses sustained by the steel fibers and by tension softening are calculated for a given crack width while the tensile stress due to tension stiffening is calculated for a given average tensile strain, the average crack spacing should be defined according to an appropriate relationship between the crack width and the average tensile strain. In this paper, the following average crack spacing model, recently derived by Deluce[33] from tests on 48 R/FRC members subjected to uniaxial tension, has been employed

$$s_{cr} = 2\left(c + \frac{s_b}{10}\right) k_3 + \frac{k_1 k_2}{s_{mi}} \tag{11}$$

where $s_b$ is the maximum spacing between reinforcing bars;

$$s_{mi} = \frac{\rho_s}{d_{bs}} + \frac{\alpha_f V_f}{d_f} \cdot \max\left(\frac{l_f / d_f}{50}, 1.0\right)$$

$c = 1.5 a_{gg}$; $k_1 = 0.4$; $k_2 = 0.25$;

$$k_3 = 1 - \frac{\min\left(V_f, 0.015\right)}{0.015} \cdot \left\{1 - \min\left(\frac{50}{l_f / d_f}, 1.0\right)\right\}$$

$a_{gg}$ is the maximum aggregate size in mm; and $\alpha_f$ is a fiber orientation factor, which can be calculated from the DEM considering member size or taken as 0.5 for an infinite member.

Figure 14 shows comparisons of the tensile behavior calculated from the proposed tension-stiffening model with results from tests performed by Bischoff[14] and Deluce and Vecchio.[17] Among the many specimens tested by Deluce and Vecchio,[17] those with a reinforcement ratio of 1.33% are shown because this reinforcement amount most closely matches values commonly found in practice. As shown in the figures, the responses computed by the proposed tension-stiffening model and the DEM showed good agreement with the test results. It should be noted once again that the good agreement for the post-yield tensile behavior indicates that the DEM predicts the tensile stress carried by the steel fibers well, while the results for the pre-yield tensile behavior indicate that the proposed tension-stiffening model reflects

the tensile stress due to the bond mechanism between the reinforcing bar and the concrete matrix well. Consequently, it can be concluded that the tensile behavior of R/FRC members can be accurately represented by the proposed tension-stiffening model and the DEM.

## CONCLUSIONS

In this paper, the tensile behavior of R/FRC members was analytically investigated on the assumption that the tensile stress resistance can be separated into three components: namely, due to the reinforcing bar, the steel fibers, and the bond mechanism between the reinforcing bar and the concrete matrix (that is, the concrete tension-stiffening effect). Unlike previous investigations in which the tension-stiffening effect was evaluated by removing only the contribution of the reinforcing bar from the total tensile stress and thus inherently including the contribution of the steel fibers, it was held in this paper that the tension-stiffening effect is only due to the bond mechanism between the reinforcing bar and the concrete matrix. Thus, the local yielding of the reinforcing bar can be reasonably detected because the distribution of the reinforcing bar stress between cracks is dominantly affected by the bond behavior of the reinforcing bar and not by the tensile stress due to steel fibers.

To derive the tension-stiffening model in R/FRC members, a newly developed crack analysis procedure considering the bond slip-stress relationship between the concrete matrix and the reinforcing bar was employed. The distribution of the tensile stress sustained by steel fibers was evaluated using the DEM. From comparisons with the results of several test specimens, it was found that the crack analysis procedure predicted both the pre-yield and post-yield tensile behavior of R/FRC members well.

An analytical parametric study was performed based on the proposed crack analysis procedure, with the steel fiber volumetric ratio, steel fiber aspect ratio, and reinforcing bar reinforcement ratio being the main variables. It was found that the tension-stiffening effect due to the bond behavior of the reinforcing bar decreased with an increase in the fiber volumetric ratio, the fiber aspect ratio, or the bond parameter of the reinforcing bar.

By extending the conventional tension-stiffening model for RC members, a simple constitutive model was developed for the tension-stiffening effect in R/FRC members. A modifying factor, allowing for the influence of steel fibers, was introduced based on the variables considered in the parametric study. Through comparisons with the test results of test specimens, it can be concluded that the proposed tension-stiffening model with the DEM predicts the tensile behavior of R/FRC members well.

The proposed tension-stiffening model can be easily implemented in a sectional or finite element analysis based on the Smeared Crack Model. Thus, it can be useful in the simulations of the behavior of FRC members or structures co-reinforced with conventional reinforcing bars subjected to not only uniaxial tension but also flexural or biaxial stress. The proposed analysis procedure is also potentially useful for various fiber types not considered in this paper. Further study is required to investigate the tension-stiffening behavior in high-performance FRC that exhibits the strain-hardening behavior.

## ACKNOWLEDGMENTS

This research was partially funded by the Basic Science Research Program through the National Research Foundation of Korea (NRF) supported by the Ministry of Education, Science and Technology (No. 20110005704); by a Nuclear Power of the Korea Institute of Energy Technology Evaluation and Planning (KETEP) grant funded by the Korean government Ministry of Knowledge Economy (No. 2011T100200162); and by the Natural Sciences and Research Council of Canada.

## NOTATION

| | | |
|---|---|---|
| $A_c$, $A_s$ | = | cross-sectional areas of concrete matrix and reinforcing bar, respectively |
| $c_f$ | = | coefficient to consider effect of steel fibers on tension-stiffening effect |
| $d_{bs}$ | = | diameter of reinforcing bar |
| $d_f$ | = | fiber diameter |
| $E_c$, $E_s$ | = | elastic modulus of concrete matrix and reinforcing bar, respectively |
| $F_c$, $F_f$, $F_s$ | = | local tension due to concrete matrix, steel fiber, and reinforcing bar, respectively |
| $f_c'$ | = | compressive strength of concrete |
| $f_c$, $f_s$ | = | local tensile stress of concrete matrix and reinforcing bar, respectively |
| $f_{cr}$ | = | cracking strength of concrete matrix |
| $f_{c,soft}$ | = | tensile stress due to tension softening |
| $f_{c,TS}$ | = | tensile stress due to tension stiffening |
| $f_f$ | = | local tensile stress due to steel fibers distributed over gross concrete section in FRC |
| $f_{s,avg}$ | = | average tensile stress of reinforcing bar |
| $f_{scr}$ | = | tensile stress of reinforcing bar at a crack |
| $f_{sy}$ | = | yield strength of reinforcing bar |
| $K_b$ | = | bond coefficient taking into account reinforcing bar strain |
| $l_f$ | = | fiber length |
| $l_t$ | = | transfer length of reinforcing bar |
| $M$ | = | bond parameter |
| $P$ | = | axial force |
| $s'$, $s''$ | = | local slip, derivative of slip, and double derivative of slip along reinforcing bar, respectively |
| $s_1$ | = | slip at bond strength |
| $s_{cr}$ | = | average crack spacing |
| $u_c$, $u_s$ | = | local deformations of concrete matrix and reinforcing bar, respectively |
| $V_f$ | = | fiber volumetric ratio |
| $w_{cr}$ | = | crack width |
| $\varepsilon_c$, $\varepsilon_s$ | = | local strains of concrete matrix and reinforcing bar, respectively |
| $\varepsilon_{scr}$ | = | local tensile strain of reinforcing bar at a crack |
| $\varepsilon_{sy}$ | = | yield tensile strain of reinforcing bar |
| $\varepsilon_{t,avg}$ | = | average tensile strain of reinforcing bar or R/FRC member |
| $\rho_s$ | = | reinforcement ratio |
| $\sigma$ | = | axial stress |
| $\tau_b$ | = | local bond stress along reinforcing bar |
| $\tau_{max}$ | = | bond strength of reinforcing bar |

## REFERENCES

1. Petersson, P. E., "Fracture Mechanical Calculations and Tests for Fiber-Reinforced Cementitious Materials," *Proceedings of Advances in Cement-Matrix Composite*s, Materials Research Society, Boston, MA, 1980, pp. 95-106.

2. Lim, T. Y.; Paramasivam, P.; and Lee, S. L., "Analytical Model for Tensile Behavior of Steel-Fiber Concrete," *ACI Materials Journal*, V. 84, No. 4, July-Aug. 1987, pp. 286-298.

3. Li, Z.; Li, F.; Chang, T.-Y. P.; and Mai, Y.-W., "Uniaxial Tensile Behavior of Concrete Reinforced with Randomly Distributed Short Fibers," *ACI Materials Journal*, V. 95, No. 5, Sept.-Oct. 1998, pp. 564-574.

4. Groth, P., "Fibre Reinforced Concrete—Fracture Mechanics Methods Applied on Self-Compacting Concrete and Energetically Modified Binders," doctoral thesis, Department of Civil and Mining Engineering, Division of Structural Engineering, Luleå University of Technology, Luleå, Sweden, 2000, 237 pp.

5. Barrangán, B. E.; Gettu, R.; Martín, M. A.; and Zerbino, R. L., "Uniaxial Tension Test for Steel Fibre Reinforced Concrete—A Parametric Study," *Cement and Concrete Composites*, V. 25, No. 7, Oct. 2003, pp. 767-777.

6. Susetyo, J., "Fibre Reinforcement for Shrinkage Crack Control in Prestressed, Precast Segmental Bridges," doctoral thesis, Department of Civil Engineering, University of Toronto, Toronto, ON, Canada, 2009, 307 pp.

7. Marti, P.; Pfyl, T.; Sigrist, V.; and Ulaga, T., "Harmonized Test Procedures for Steel Fiber-Reinforced Concrete," *ACI Materials Journal*, V. 96, No. 6, Nov.-Dec. 1999, pp. 676-686.

8. Voo, J. Y. L., and Foster, S. J., "Variable Engagement Model for Fibre Reinforced Concrete in Tension," Uniciv *Report* No. R-420, School of Civil and Environmental Engineering, The University of New South Wales, New South Wales, Australia, June 2003, 86 pp.

9. Lee, S.-C.; Cho, J.-Y.; and Vecchio, F. J., "Diverse Embedment Model for Fiber-Reinforced Concrete in Tension: Model Development," *ACI Materials Journal*, V. 108, No. 5, Sept.-Oct. 2011, pp. 516-525.

10. Lee, S.-C.; Cho, J.-Y.; and Vecchio, F. J., "Diverse Embedment Model for Fiber-Reinforced Concrete in Tension: Model Verification," *ACI Materials Journal*, V. 108, No. 5, Sept.-Oct. 2011, pp. 526-535.

11. Lee, S.-C.; Cho, J.-Y.; and Vecchio, F. J., "Model for Post-Yield Tension Stiffening and Rebar Rupture in Concrete Members," *Engineering Structures*, V. 33, No. 5, May 2011, pp. 1723-1733.

12. Abrishami, H. H., and Mitchell, D., "Influence of Steel Fibers on Tension Stiffening," *ACI Structural Journal*, V. 94, No. 6, Nov.-Dec. 1997, pp. 769-776.

13. Noghabai, K., "Behavior of Tie Elements of Plain and Fibrous Concrete and Varying Cross Sections," *ACI Structural Journal*, V. 97, No. 2, Mar.-Apr. 2000, pp. 277-285.

14. Bischoff, P. H., "Tension Stiffening and Cracking of Steel Fiber-Reinforced Concrete," *Journal of Materials in Civil Engineering*, ASCE, V. 15, No. 2, Apr. 2003, pp. 174-182.

15. Chiaia, B.; Fantilli, A. P.; and Vallini, P., "Evaluation of Crack Width in FRC Structures and Application to Tunnel Linings," *Materials and Structures*, V. 42, No. 3, Apr. 2009, pp. 339-351.

16. Na, C., and Kwak, H.-G., "A Numerical Tension-Stiffening Model for Ultra High Strength Fiber-Reinforced Concrete Beams," *Computers and Concrete*, V. 8, No. 1, Feb. 2011, pp. 1-22.

17. Deluce, J. R., and Vecchio, F. J., "Cracking of SFRC Members Containing Conventional Reinforcement," *ACI Structural Journal*, V. 110, No. 3, May-June 2013, pp. 481-490.

18. Vecchio, F. J., and Collins, M. P., "The Modified Compression Field Theory for Reinforced Concrete Elements Subjected to Shear," *ACI Journal*, V. 83, No. 2, Mar.-Apr. 1986, pp. 219-231.

19. Vecchio, F. J., "Disturbed Stress Field Model for Reinforced Concrete: Formulation," *Journal of Structural Engineering*, ASCE, V. 126, No. 9, Sept. 2000, pp. 1070-1077.

20. Vecchio, F. J., "Disturbed Stress Field Model for Reinforced Concrete: Implementation," *Journal of Structural Engineering*, ASCE, V. 127, No. 1, Jan. 2001, pp. 12-20.

21. Bentz, E. C., "Sectional Analysis of Reinforced Concrete Members," doctoral thesis, Department of Civil Engineering, University of Toronto, Toronto, ON, Canada, 2000, 184 pp.

22. Ramaswamy, A.; Barzegar, F.; and Voyiadjis, G. Z., "Postcracking Formulation for Analysis of RC Structures Based on Secant Stiffness," *Journal of Engineering Mechanics*, ASCE, V. 120, No. 12, Dec. 1994, pp. 2621-2640.

23. Ramaswamy, A.; Barzegar, F.; and Voyiadjis, G. Z., "Study of Layering Procedure in Finite-Element Analysis of RC Flexural and Torsional Elements," *Journal of Structural Engineering*, ASCE, V. 121, No. 12, Dec. 1995, pp. 1773-1783.

24. Wong, P. S., and Vecchio, F. J., "VecTor2 & FormWorks User's Manual," *Publication No. 2002-02*, Department of Civil Engineering, University of Toronto, Toronto, ON, Canada, Aug. 2002, 214 pp.

25. Balázs, G. L., "Cracking Analysis Based on Slip and Bond Stresses," *ACI Materials Journal*, V. 90, No. 4, July-Aug. 1993, pp. 340-348.

26. Oh, B. H., and Kim, S. H., "Advanced Crack Width Analysis of Reinforced Concrete Beams under Repeated Loads," *Journal of Structural Engineering*, ASCE, V. 133, No. 3, Mar. 2007, pp. 411-420.

27. Harajli, M.; Hamad, B.; and Karam, K., "Bond-Slip Response of Reinforcing Bars Embedded in Plain and Fiber Concrete," *Journal of Materials in Civil Engineering*, ASCE, V. 14, No. 6, Dec. 2002, pp. 503-511.

28. CEB-FIP MC90, "Model Code for Concrete Structures," Comité Euro-International du Béton-Fédération Internationale, Thomas Telford, London, UK, 1990, 437 pp.

29. Ruiz, M. F.; Muttoni, A.; and Gambarova, P. G., "Analytical Modeling of the Pre and Postyield Behavior of Bond in Reinforced Concrete," *Journal of Structural Engineering*, ASCE, V. 133, No. 10, Oct. 2007, pp. 1364-1372.

30. Bentz, E. C., "Explaining the Riddle of Tension Stiffening Models for Shear Panel Experiments," *Journal of Structural Engineering*, ASCE, V. 131, No. 9, Sept. 2005, pp. 1422-1425.

31. CSA A23.3-04, "Design of Concrete Structures," Canadian Standards Association, Mississauga, ON, Canada, 2004, 214 pp.

32. Mansur, M. A.; Chin, M. S.; and Wee, T. H., "Stress-Strain Relationship of High-Strength Fiber Concrete in Compression," *Journal of Materials in Civil Engineering*, ASCE, V. 11, No. 1, Feb. 1999, pp. 21-29.

33. Deluce, J. R., "Cracking Behaviour of Steel Fibre Reinforced Concrete Containing Conventional Steel Reinforcement," master's thesis, Department of Civil Engineering, University of Toronto, Toronto, ON, Canada, 2011, 469 pp.